Appendix 1

Supplementary Method 1: acquisition protocol of dynamic contrast-enhanced magnetic resonance imaging

All patients enrolled in this study underwent preoperative breast magnetic resonance imaging (MRI) scanning before surgery for primary and recurrent tumors. The 1.5-T or 3.0-T MR scanners manufactured by Aurora (Espoo, Finland), GE Healthcare (Chicago, IL, USA), and Siemens Healthineers (Erlangen, Germany) were used to generate breast MR images in heterogeneous parameters (*Table S1*). Dynamic contrast-enhanced MRI (DCE-MRI) was conducted, and the resulting images were used for analysis.

Supplementary Method 2: determination of qualitative characteristics and extraction of quantitative features in MR images

Qualitative characteristics

MR images were reviewed by two radiologists (reader 1 and reader 2) with 9 and 1 years of experience in breast MRI, respectively. They were blinded to the patient outcomes. The following qualitative and conventional characteristics were determined via the review of all MRI scans in consensus of the two radiologists based on the Breast Imaging Reporting and Data System (BI-RADS) lexicon: background parenchymal enhancement (BPE) levels (minimal, mild, moderate, or marked), amounts of fibroglandular tissue (FGT; almost entirely fat, scattered FGT, heterogeneous FGT, or extreme FGT), lesion type, lesion morphology, absence or presence of multifocal/multicenter disease, and peritumoral edema. In patients with multiple lesions, the findings of the largest tumor were evaluated. For BPE determination, we relied on the amount of FGT enhancement on initial contrast-enhanced or subtraction images and maximum-intensity projection images (37). The multifocal disease was defined as findings suggestive of additional sites of malignancy in the same breast quadrant or less than 4 cm away from the index lesion, while multicentric disease was defined as findings suggestive of additional sites of malignancy in different quadrants of the ipsilateral breast or more than 4 cm away from the index lesion (38). Peritumoral edema was defined when high signal intensity around the tumor or posterior to the tumor mass in the prepectoral area was observed on T2-weighted images (39).

Extraction of quantitative features

The regions of interest (ROIs) and the contour of the tumor on the peak enhanced phase of DCE-MRI were manually and independently segmented via ITK-Snap software (version 4.0) by two radiologists (reader 1 and reader 2) who were blinded to the clinicopathologic information and outcome of patients. The open-source PyRadiomics package (version 3.0) was used to conduct feature extraction and image preprocessing. Before feature extraction, image normalization was performed to alleviate the bias caused by the varied imaging parameters in this study. The normalization algorithms employed have been used and verified in our previous studies (34,40). First, all voxel sizes of the images were resampled to $1\times1\times2$ mm^3 using the B-spline interpolation algorithm. Furthermore, Z-score normalization was applied to standardize the grayscale values of the images to make them consistent. To ensure more dependable results with the limited sample size, we focused solely on extracting original radiomics features rather on than higher-dimensional ones. Ultimately, a total of 204 quantitative features were extracted from the first-phase DCE-MRI of both primary and recurrent tumors, with 102 features extracted from each. These features could be grouped as (I) shape features, (II) first-order histogram-based features, and (III) texture features. The textural features described the intrinsic heterogeneous texture of the tumor lesion based on 4 textural matrixes: the gray-level co-occurrence matrix (GLCM), the gray-level run-length matrix (GLRLM), the gray-level size zone matrix (GLSZM), and the gray-level dependence matrix (GLDM). Since there was a lack of consistency in MRI scanners, only original image features were extracted and not other high-dimensional features such as wavelet transform. Finally, we extracted 204 quantitative features on the tumor lesion area consisting of shape and size features (14×2), first-order histogram-based features (18×2), and textural features (70×2) for the original image of primary and recurrent tumor.

© Quantitative Imaging in Medicine and Surgery. All rights reserved.
https://dx.doi.org/10.21037/qims-23-1831

Table S1 The imaging parameters of different DCE-MRI machines

MRI machine	Magnetic intensity (T)	Dosage of Gd-DTPA (mmol/kg)	Time of repetition (ms)	Time of echo (ms)	Field of view (mm×mm)	Slice thickness (mm)	Gap (mm)	Flip angle
Aurora	1.5	0.1	29	4.8	360×360	1.48	0	90°
GE	1.5	0.2	5	2.4	280×280	2.6	0	12°
GE	3	0.1	4	2.1	300×300	4	0	10°
Siemens	3	0.1	4.5	1.56	360×360	2.2	0	10°

DCE-MRI, dynamic contrast-enhanced magnetic resonance imaging.

Table S2 The list of patients with distant metastasis

ID	Distant metastasis site	Pathology
P1	Lung	Invasive carcinoma
P2	Bone	Invasive carcinoma
P3	Bone	Invasive carcinoma
P4	Brain	Invasive carcinoma
P5	Lung	Invasive carcinoma
P6	Distant lymph nodes	Invasive carcinoma
P7	Lung	Invasive carcinoma
P8	Bone and distant lymph nodes	Invasive carcinoma
P9	Liver and distant lymph nodes	Invasive carcinoma
P10	Lung	Invasive carcinoma
P11	Lung and distant lymph nodes	Invasive carcinoma
P12	Bone	Invasive carcinoma
P13	Lung	Invasive carcinoma
P14	Distant lymph nodes	Invasive carcinoma
P15	Lung	Metaplastic carcinoma

© Quantitative Imaging in Medicine and Surgery. All rights reserved.
https://dx.doi.org/10.21037/qims-23-1831

Table S3 Univariable Cox regression analyses of factors associated with DMFS for patients with IBTR

Variable of primary and recurrent tumor	Univariable	
	Hazard ratio (95% CI)	P value
Presentation at primary cancer		
Age (versus ≥40 years)		
<40 years	2.44 (0.88–6.67)	0.09
Tumor size (versus ≤20 mm)		
>20 mm	1.22 (0.44–3.38)	0.70
LN (versus negative)		
Positive	2.52 (0.91–7.02)	0.08
Histological grade (versus grade I or II)		
Grade III	2.16 (0.59–7.87)	0.24
Unknown	2.22 (0.37–13.3)	0.38
LVI (versus no)		
Yes	1.54 (0.54–4.33)	0.42
ER status (versus negative)		
Positive	1.8 (0.65–4.98)	0.26
PR status (versus negative)		
Positive	1.49 (0.54–4.11)	0.44
HER2 status (versus positive)		
Negative	3.13 (0.88–11.1)	0.08
Ki-67 index (versus >20%)		
≤20	1.59 (0.44–5.56)	0.48
Chemotherapy (versus no)		
Yes	4.71 (0.62–35.9)	0.14
Radiotherapy (versus no)		
Yes	1.63 (0.52–5.12)	0.40
Endocrine therapy (versus no)		
Yes	1.26 (0.35–4.5)	0.73
Anti-HER2 therapy (versus yes)		
No	2.94 (0.39–25)	0.29
FGT (versus almost entirely fat or scattered)		
Heterogeneous or extreme	1.92 (0.61–6.01)	0.26
BPE (versus minimal or mild)		
Moderate or marked	1.89 (0.69–5.23)	0.22
Lesion type (versus ME)		
NME	1.19 (0.40–3.55)	0.76
Both	0.46 (0.06–3.65)	0.54
Multifocal disease (versus absent)		
Present	0.91 (0.31–2.68)	0.87
Peritumoral edema (versus absent)		
Present	1.18 (0.43–3.25)	0.76
Presentation at IBTR		
DFI (versus >2 years)		
≤2 years	2.08 (0.66–6.67)	0.21
Tumor size (versus ≤20 mm)		
>20 mm	2.45 (0.87–6.94)	0.09
Resection (versus mastectomy)		
Lumpectomy	1.19 (0.27–5.26)	0.82
Histological subtype (versus ductal)		
Not ductal	2.55 (0.56–11.7)	0.23
Histological grade (versus grade I or II)		
Grade III	1.50 (0.41–5.45)	0.54
Unknown	0.47 (0.08–2.83)	0.41
ER status (versus negative)		
Positive	1.1 (0.37–3.2)	0.88
PR status (versus negative)		
Positive	2.94 (0.38–20)	0.30
HER2 status (versus positive)		
Negative	3.23 (1.01–10)	0.048*
Ki-67 index (versus ≤20%)		
>20	1.65 (0.52–5.19)	0.39
Chemotherapy (versus no)		
Yes	2.29 (0.51–10.2)	0.28
Radiotherapy (versus no)		
Yes	1.71 (0.38–7.59)	0.48
Endocrine therapy (versus no)		
Yes	1.09 (0.37–3.18)	0.88
Anti-HER2 therapy (versus yes)		
No	1.41 (0.45–4.35)	0.56
FGT (versus almost entirely fat or scattered)		
Heterogeneous or extreme	2.21 (0.49–9.86)	0.30
BPE (versus minimal or mild)		
Moderate or marked	4.22 (1.42–12.5)	0.01*
Lesion type (versus ME)		
NME	0.59 (0.16–2.14)	0.42
Both	1.35 (0.29–6.25)	0.7
Multifocal disease (versus absent)		
Present	0.84 (0.29–2.47)	0.84
Peritumoral edema (versus absent)		
Present	1.87 (0.67–5.27)	0.23

*, P<0.05. DMFS, distant metastasis-free survival; IBTR, ipsilateral breast tumor recurrence; CI, confidence interval; LN, lymph node; LVI, lymphovascular invasion; ER, estrogen receptor; PR, progesterone receptor; HER2, human epidermal growth factor receptor 2; DFI, disease-free interval; FGT, fibroglandular tissue; BPE, background parenchymal enhancement; ME, mass enhancement; NME, nonmass enhancement.

© Quantitative Imaging in Medicine and Surgery. All rights reserved.
https://dx.doi.org/10.21037/qims-23-1831

Table S4 Prognostic performance of combined model compared with other models

Model	Time-dependent AUC			P value		
	2 years	3 years	5 years	2 years	3 years	5 years
Clinicoradiological	0.72	0.76	0.71	Ref.	Ref.	Ref.
Radiomics	0.80	0.82	0.88	0.48	0.63	0.27
Combined	0.84	0.89	0.90	0.06	0.05	0.07

AUC, area under the curve; Ref. reference.

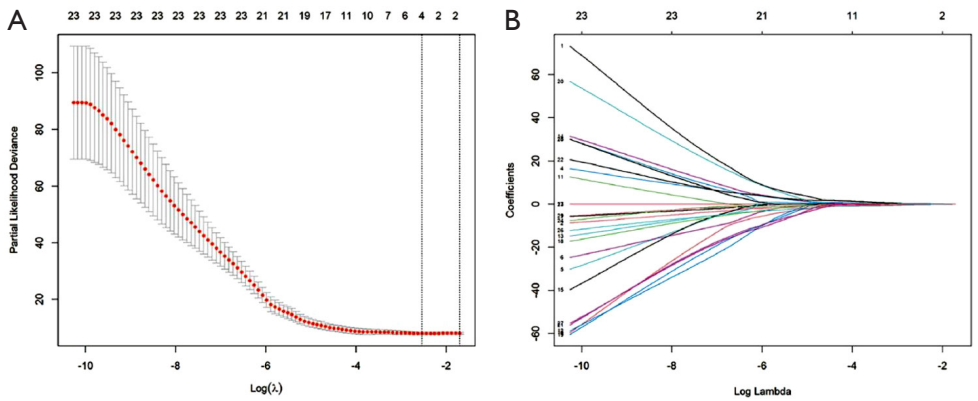

Figure S1 Quantitative feature selection using the LASSO Cox regression model. (A) The partial likelihood deviance was plotted versus log (lambda). The y-axis indicates the partial likelihood deviance, while the lower x-axis indicates the log (lambda), and the upper x-axis represents the average number of predictors. Dotted vertical lines were drawn at the optimal values using the minimum criteria and 1 standard error of the minimum criteria. The tuning parameter (λ) was selected in the LASSO model via 10-fold cross-validation based on minimum criteria. (B) LASSO coefficient profiles of the 29 quantitative features for recurrent tumor. The coefficients (y-axis) were plotted against log (lambda) and 4 features with nonzero coefficients were selected to build the quantitative signature. LASSO, least absolute shrinkage and selection operator.

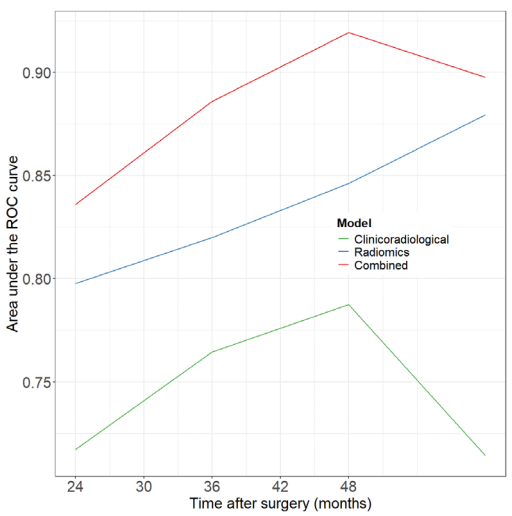

Figure S2 Time-dependent area under ROC curve of the clinicoradiological model, radiomics model, and combined model for DMFS prediction. The combined model had the best performance compared with both the clinicoradiological model and radiomics model at various time points. ROC, receiver operating characteristic; DMFS, distant metastasis-free survival.

© Quantitative Imaging in Medicine and Surgery. All rights reserved.
https://dx.doi.org/10.21037/qims-23-1831

References

37. Dontchos BN, Rahbar H, Partridge SC, Korde LA, Lam DL, Scheel JR, Peacock S, Lehman CD. Are Qualitative Assessments of Background Parenchymal Enhancement, Amount of Fibroglandular Tissue on MR Images, and Mammographic Density Associated with Breast Cancer Risk? Radiology 2015;276:371-80.
38. Bae MS, Lee SH, Chu AJ, Shin SU, Ryu HS, Moon WK. Preoperative MR Imaging in Women with Breast Cancer Detected at Screening US. Radiology 2017;282:681-9.
39. Uematsu T, Kasami M, Watanabe J. Is evaluation of the presence of prepectoral edema on T2-weighted with fat-suppression 3 T breast MRI a simple and readily available noninvasive technique for estimation of prognosis in patients with breast cancer? Breast Cancer 2014;21:684-92.
40. Su GH, Xiao Y, You C, Zheng RC, Zhao S, Sun SY, Zhou JY, Lin LY, Wang H, Shao ZM, Gu YJ, Jiang YZ. Radiogenomic-based multiomic analysis reveals imaging intratumor heterogeneity phenotypes and therapeutic targets. Sci Adv 2023;9:eadf0837.

© Quantitative Imaging in Medicine and Surgery. All rights reserved.
https://dx.doi.org/10.21037/qims-23-1831